Permanent Magnet Excited Generator For Gearless Wind Generation Plant

Paul Curiac*, D.H.Kang, D.Y.Park
(K.R.E.I)

Abstract - This paper presents an axial flux permanent magnet synchronous generator with a high power-to-weight ratio, dedicated for small-scale gearless wind power generation plants. For this purpose, a specific design is necessary to meet the imposed requirements. In this paper the design technique for the specifications is presented. The aim of the paper is also to discuss some of the first obtained test results and the involved demagnetizing problem (i.e. short-circuit).

Keywords : permanent magnet synchronous generator, axial flux machine.

1. INTRODUCTION

The recent advancements of permanent magnet (PM), soft magnetic materials, solid-state devices and electronics have contributed to new energy efficient, high performance electric drives for modern PM machines. Owing to rare-earth PMs, these machines have higher efficiency, power factors, output power per mass and volume, and better dynamic performance than other electrical machines.

Nowadays, for example, the PM axial flux machines are an attractive candidate for wind generation plant, electrical vehicles and ship propulsion systems especially because of the before mentioned qualities and the simple mechanical configuration [1]. Thus, the wind turbine system with direct-driven axial PM synchronous generator (APMSG) can avoid a gear box which is necessary for conventional generators; this kind of machine is short, and has a large diameter to get a large torque, which otherwise would be generated by the gear box [2].

Axial flux or disk-type PM machines can be designed with or without armature slots, with internal or external PM rotors and with surface mounted or interior type PMs; the control of axial flux disk machines is identical to that of PM synchronous machines of cylindrical construction.

In the double-sided machine with internal PM disk rotor, the armature winding is located on two stator cores as shown in Fig.1. The disk with PMs rotates between two stator cores; thus, the internal type machine allows higher torque density in comparison with the external type machine.

In order to obtain a new design, which combines high efficiency with high power, a first experimental APMSG dedicated to small - scale wind power generation plant [3] is built and tested.

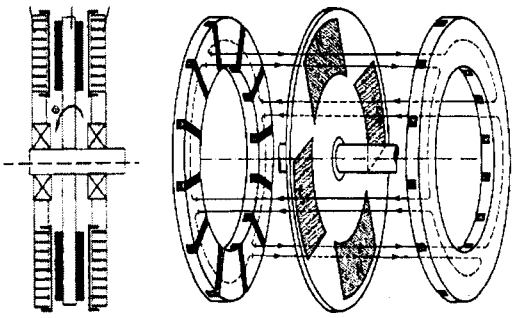

Figure 1. Internal disk type APMSG [4]

2. MACHINE STRUCTURE

The machine is built having two stators and one disk type rotor as shown in Figs. 1 and 2. Each toroidal stator core is wound with a continuous electro-technical steel tape and the slots are shaped by machining; each stator cores ring structure has open slots on one side. The three-phase stator windings are mounted into the slots. The two stators are symmetrically fixed on the mechanical frame and the rotor is realized by hard aluminum alloy disk form, fixed to the shaft between the two stators, and carrying the axially magnetized magnets.

The magnets are put into holes in the rotor disc; both the disc and the magnets have the same thickness. Two pole shoes are mechanically fixed on the opposite surfaces of every permanent magnet; thus, the fixed pole shoes help the rotor to have robust structure. Fig. 2 shows the rotor disk with the PMs fixed axially between the two mild steel poles shoes.

Fig. 3 shows the two stators; the first one, at left, is in the final form - after its impregnation by complete immersion - and the second one, at right, before impregnation process.

The machine parameters are summarized in Table 1.

Figure 2. The rotor(left) and startor(right) of APMSG

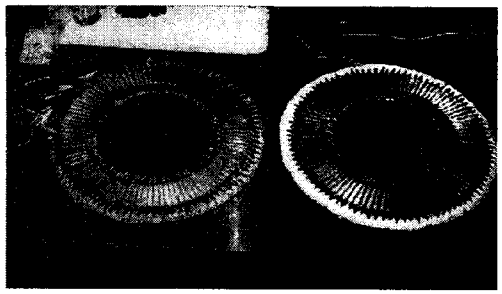

Figure 3. Two stators of APMSG

Table 1. Machine Parameters

Rated power	2500	VA
Rated speed	250	rpm
Rated voltage	380	V
Rated power factor (cos ϕ)	0.8	
No. of poles	24	
No. of phases	3	
No. of slots/pole/phase		13/8
Remanence	1.0	T
Rated current density	4.0	A/mm^2
Airgap length	2 × 1	mm
Inner diameter	322	mm
External diameter	410	mm

3. DESIGN CONSIDERATIONS

3.1 Armature winding

This first constructed machine operates in a generating mode. In order to reduce the harmonics in the magnetic flux and the electromotive force, the machine is designed to have a three-phase, double-layer lap armature winding with fractional number of slots per pole per phase [4] as shown in Table 1.

3.2. Losses & efficiency

The *iron losses* in the teeth, PFet, and in the stator yoke, PFey, are determined by the following equations:

$$P_{Fet} = k_t v_{10} [f/50]^{1.8} m_t B_t^2 \quad (1)$$

$$P_{Fey} = k_y v_{10} [f/50]^{1.8} m_y B_y^2 \quad (2)$$

$$k_t = k_y = 1.6 \quad (3)$$

$$v_{10} = 2.4 \frac{W}{kg} \quad (4)$$

$$P_{Fe} = P_{Fet} + P_{Fey} \quad (5)$$

where f is the frequency, v_{10} is the specific core loss at 1 T and 50 Hz, m_t and m_y are the overall mass of the teeth and the yoke, and B_t, B_y the flux densities of the teeth and the yoke, respectively [2].

The *additional loss*, P_{add}, is estimated to be 0.5% of the nominal power according to IEC 34-2.

$$P_{add} = 0.005 P_N \quad (6)$$

The *ohmic losses*, P_{Cu}, of the stator winding is calculated at a temperature of 90 °C as in eqn. (7).

$$P_{Cu} = \rho_{Cu90} V_{Cu} J^2 \quad (7)$$

where V_{Cu} is the overall volume of the copper winding, J is the armature current density, and ρ_{Cu90} is the specific resistance.

Friction losses is neglected due to the low speed. Therefore the efficiency η is obtained as in eqn. (8).

$$\eta = \frac{P}{P_{iN}} \frac{P_e - P_{Cu}}{P_e + P_{add} + P_{Fe}} \quad (8)$$

where the input power is calculated by adding the electromagnetic power P_e and the sum of iron and additional losses, P_{Fe} and P_{add}.

In the first approximation, because of the stator winding type, the efficiency is calculated by the electromagnetic power instead of the internal power. The electromagnetic power can be calculated by Fourier analysis of B_δ along the air-gap, yielding the fundamental field amplitude $B_{\delta 1}$ (the radial component of air-gap flux density) in no-load operating condition. The electromagnetic power as functions of induced EMF, E_f, and current, I_a, is

$$P_e = 3E_f I_{aq} = 3E_f I_a \cos \Psi \quad (9)$$

where the angle $\Psi = \phi - \delta$ (δ :load angle) [1].

3.3. Axial Force

Assuming sinusoidally distributed flux density B and electric loading J, the torque T is given by

$$T = \pi J R_i \left(R_e^2 - R_i^2\right) B \tag{10}$$

and the axial force between the rotor disc and one stator is

$$F = \frac{\pi(R_e^2 - R_i^2) B^2}{4\mu_0} \tag{11}$$

where B and J are peak values and R_i and R_e are the inner and outer radii of the stator core (R_e=205 mm, R_i=161 mm), respectively. The force is estimated to be larger than 7000 N for each stator.

4. MODELING OF APMSG

The winding inductances and the induced electromotive force (EMF) can be calculated using a three dimensional analysis. The magnetic model can be simplified to a two dimensional one by introducing a cylindrical cutting plane at the mean radius of the magnets; this axial section is unfolded into a 2D surface on which the finite element method (FEM) analysis can be performed.

The magnetostatic field problem of the APMSGs may be solved on the basis of the following vector equation

$$\nabla \times (\nu \cdot \nabla \times A) \cdot \nabla \times \nu \times B_r = 0 \tag{12}$$

where **A** is the magnetic vector potential, is the reluctivity given by $|Hc/Br|$, **Br** is the remanent magnetic flux density, and **Hc** is the coercive magnetic flux of the PM.

Based on the minimization of an energy functional, the FEM discretization procedure transforms the partial differential eqn.(12) into a number of simultaneous, nonlinear algebraic equations containing the unknown node potentials. To solve the equations, iterations are essential and the NewtonRaphson and conjugategradient procedures are used [4].

Because of the unsymmetry of the magnetic circuit and complex electric configuration (the three-phase, double-layer lap armature winding with fractional number of slots per pole per phase), an integer 2D field calculation model is constructed. Thus, Fig. 4 shows the no-load magnetic flux distribution for one relative position of the stator-rotor, and Fig. 5 presents the airgap magnetic flux density waveform at the axial section on the stator average diameter.

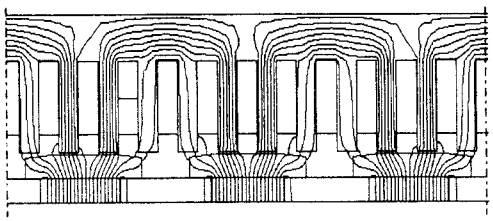

Figure 4. No-load magnetic flux distribution (partial view)

The magnetic flux density variations in the middle of the airgaps of three axial planes (at radii of 172, 183, and 194 mm) of the machine are harmonically analyzed by developing them in Fourier series. The average harmonics spectrum is shown in Fig. 6. Fig. 7 shows the harmonics spectrum of the induced EMF.

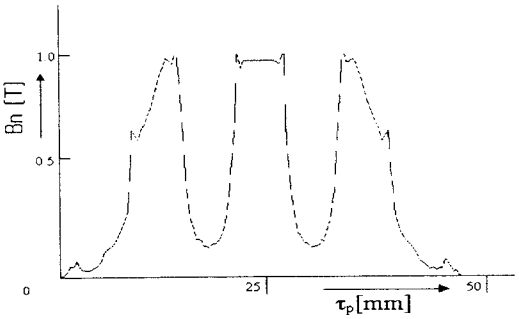

Figure 5. Airgap magnetic flux density for a polar path

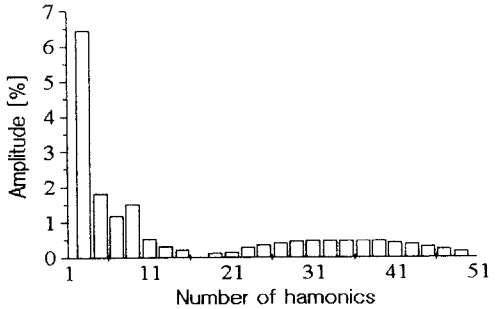

Figure 6. No-load FEM analysis: harmonics spectrum of the airgap magnetic flux density curve

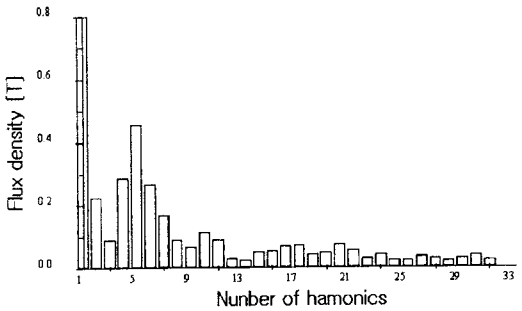

Figure 7. Harmonics spectrum of EMF

5. ACCIDENTAL DEMAGNETIZING

In order to prevent the magnetic material from demagnetizing in case of a short circuit, it is necessary to estimate the magnetic field strength within the magnet. An approximate value of the largest fault current, I_K (the short circuit current), can be obtained by EMF, E_f, and synchronous reactance, X_{sd} as in (13).

$$I_K = 2 \frac{E_f}{X_{sd}} \tag{13}$$

Thus, the ampere-turns, Θ_a,of the armature are

$$\Theta_a = \frac{w}{p} I_k \frac{\sqrt{3}}{2} \tag{14}$$

where w is the number of turns per phase and p is the number of pole-pairs.
In case of non-saturated iron, the magnetic field strength within the magnet, HM, is given by [2],

$$H_M = \frac{\mu_0 \frac{\Theta_a}{\delta} - B_r}{B_{rover} H_c + \mu_0 \frac{h_M}{\delta}} \tag{15}$$

where δ is the air-gap, h_M is PMs height.
Hence, the condition for demagnetization is:

$$|H_M| < |H_C| \tag{16}$$

6. TEST RESULTS

Tests of the APMSG demonstrate satisfactory results so far. Fig. 8 shows, comparatively with Fig. 7, the experimentally obtained harmonics spectrum, which is determined by frequency analysis for one phase of the machine; the wye connected stator winding itself cancels the EMFs third harmonics from the line-to-line EMF, and no thirdharmonic current can flow provided that the star point of the winding is isolated.

Fig. 9 shows the output voltage-current curves (the external characteristics) at the rated power factor, and it can be seen that the specified output is met correctly. The measured temperature rise at full load is modest and the efficiency is over 85 %.

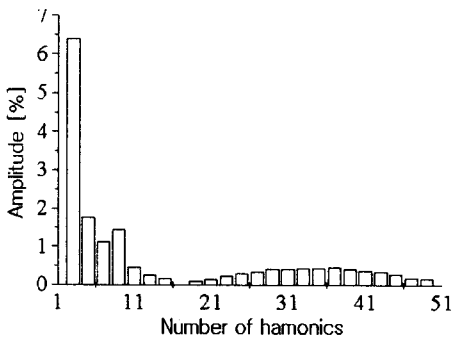

Figure 8. Measured harmonics spectrum of the induced electromotive force

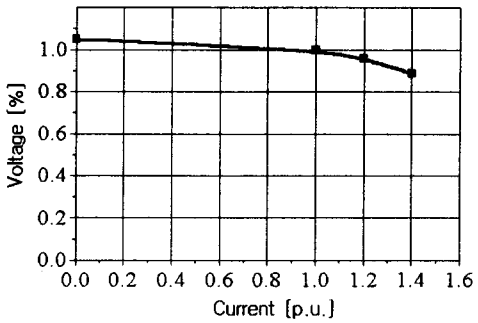

Figure 9. Measured external characteristics of APMSG

7. CONCLUSIONS

A very compact APMSG having the excellent thermal properties could be built due to the combination of new magnetic material of very high strength and the properly designed winding configuration.

Basic tests confirm that the APMSGs measured parameters met the main design specifications. Thus, the no-load terminal voltage and the rated voltage at rated current, rated power factor, and rated speed have both the expected values; measured harmonics spectrum shows that the output voltage wave shape is close to a sinusoid.

The APMSG has a simple design and is easy to build: therefore if it is needed to increase the delivered power of one machine while keeping the same diameter, it could be used as one module of a large power generator by axially adding up.

8. REFERENCES

[1] J. F. Gieras, M. Wing, Permanent Magnet Motor Technology, Marcel Dekker, Inc., New York, 1997

[2] Ch. Schaetzer, a.o. Vector Optimization of Two-dimensional Numerical Field Problems Applied to the Design of a Wind Turbine Generator , IGTE98, Graz, Austria, Sept. 1998

[3] C. Bala, P. Curiac, V. Lupu, D. Popescu, PMs Synchronous Generators for Power Generation Equipments , The Second Biennial Int. Conf. on Applied Electr., PUB, Bucharest, Dec. 1997 (in Romanian).

[4] Z. Zhang, F. Profumo, A. Tenconi, Design of an Axial Flux Interior PM Synchronous Motor , ICEM98, Istanbul, Turkey, Sept. 1998